Polymer 51 (2010) 1972–1982

Contents lists available at ScienceDirect

Polymer

journal homepage: www.elsevier.com/locate/polymer

Rheological properties of guar and its methyl, hydroxypropyl and hydroxypropyl-methyl derivatives in semidilute and concentrated aqueous solutions

Daniela Risica [a], Andrea Barbetta [a], Luca Vischetti [a], Cesare Cametti [b,c], Mariella Dentini [a,*]

[a] Department of Chemistry, University of Rome "La Sapienza", Rome, Italy
[b] Department of Physics, University of Rome "La Sapienza", Rome, Italy
[c] INFM-CNR CRS-SOFT, Italy

ARTICLE INFO

Article history:
Received 15 December 2009
Received in revised form
22 February 2010
Accepted 23 February 2010
Available online 3 March 2010

Keywords:
Guar derivatives
Light scattering
Rheology

ABSTRACT

We report on a comparative study of the rheological properties of guar [GG], methyl guar [MG], hydroxypropyl guar [HPG] and hydroxypropyl-methyl guar [MHPG] polymers aqueous solutions in semidilute (both unentangled and entangled) and concentrated regimes, using oscillatory and steady-shear techniques. In the dilute regime, molecular weights and radii of gyration have been investigated by means of light scattering measurements.

Data obtained from steady-shear rheology were satisfactorily analyzed according to Cross model and the effects of polymer concentration and temperature on the rheological behaviour of guar and guar derivatives have been investigated and discussed in terms of rheological parameters, such as the zero-shear viscosity η_0, the characteristic time τ and critical coil-overlap concentration C^*.

The storage and loss moduli of guar and guar derivatives aqueous solutions have been measured using angular frequencies in the range between 10^{-3} and 10 rad/s. The data have been analyzed using the "blob" model for semidilute solutions and the scaling approach proposed by Rubinstein, Dobrynin and Colby for concentrated solutions. These rheological parameters obey a time–concentration superposition principle, so that master curves can be constructed over a wide frequency range. Moreover, we show that, at lower temperatures, these systems behave as thermo-rheological simple systems, in that the oscillatory shear response at different temperatures can be superimposed according to the empirical time–temperature superposition principle. Although these systems can be conveniently described within a unifying scaling model, the behaviour of guar derivatives are somewhat different. At higher temperatures, relatively small deviations from the scaling behaviour of the storage modulus of MG and MHPG polymers were observed. These findings can be justified by a structural re-organization of the macromolecular network, due to the hydrophobic interactions.

1. Introduction

Guar-gum [GG] is a polysaccharide originating from the seed endosperm of the plant Cyamopsis tetragonolobus. It is a galactomannan, which consists of a (1 → 4)-linked β-D-mannopyranosyl backbone partially substituted at O-6 with α-D-galactopyranosyl side groups, with the ratio of mannose to galactose of about 1.6–1.8 [1]. This polysaccharide has been extensively used in a wide range of applications because of its unique ability to alter the rheological properties, the thickening and the viscosity of aqueous solutions [2,3].

The unusually high viscosities of guar-gum are the result of its large hydrodynamic volume in solution and of the nature of its specific intermolecular interactions (entanglements). Because of its availability and manufacture easiness, guar-gum is one of the most effective natural thickener. Guar-gum products show a pronounced temperature thinning effect when their solutions are heated. This is caused by loss of water of hydration around the polymer molecule and by an increased flexibility of the polymer chain. Lost viscosity is regained upon cooling.

However, incomplete hydration of guar-gum at room temperatures, poor clarity of the solution and the desire for products with modified or particular properties have led to the development of a variety of commercial ether derivatives. In the commercial production, guar or guar endosperm is generally reacted in

* Corresponding author. Tel.: +39 (0) 6 49913633; fax: +39 (0) 6 490631.
E-mail address: mariella.dentini@uniroma1.it (M. Dentini).

0032-3861/$ – see front matter © 2010 Elsevier Ltd. All rights reserved.
doi:10.1016/j.polymer.2010.02.041

heterogeneous processes using water, organic solvent, or both, in a slurry media. As in the production of cellulose ethers, aqueous bases are employed to swell the gum allowing a good penetration of reactants, achieving a uniform substitution and favouring the removal of reaction by-products.

Native guar-gum has been chemically modified into various water-soluble derivatives by using reactive functional groups to substitute free hydroxyl groups along the macromolecular backbone, in order to broaden its industrial applications, such as in food, paints and pigments, oilfield, mining, paper, water treatment, personal care and in pharmaceuticals and agriculture. For instance, the conversion of guar galactomannan to the hydroxypropyl derivative results in a product having much less insoluble residue than the parent guar, as well as a better temperature stability and solubility in solution. In biological applications, guar-gum and modified guar-gum were used as a carrier for colon targeted [4] and transdermal drug delivery system [5]. Furthermore, besides a faster and better solubility in water, multifunctional characteristics can be obtained for this biomacromolecule by the introduction of ionic substituents [6].

However, in spite of the industrially important applications and the relevant scientific interest, studies of the rheological behaviour of such hydrophobized guar derivatives are scarce and thereby a wide rheological knowledge is not fully available. On the other hand, knowledge of the rheological behaviour of guar-gum and its various derivatives in aqueous solutions is essential for meeting end-user requirements.

In a previous paper [7], we have presented a study of the influence of the increasing level of methyl substitution on guar chain flexibility, as reflected by its dilute solution properties. The aim of the present paper is to extend that previous work towards a systematic investigation of the shear and time-dependent viscosity properties of guar [GG], methyl guar [MG], hydroxypropyl guar [HPG] and hydroxypropyl-methyl guar [MHPG] polymer aqueous solutions, in order to evaluate the effect of polymer concentration, degree of hydrophobic substitution and temperature on the rheological behaviour of these systems.

2. Experimental

2.1. Materials

Guar-gum [GG], hydroxypropyl guar [HPG] with a degree of substitution of 1.2 and hydroxypropyl-methyl guar [MHPG] with a molar substitution of 0.4 and degree of substitution of 1.2 were supplied by Lamberti s.p.a. (Plant and Technological Centre of Albizzate, Italy). The synthesis of methoxyl guar [MG] has been described previously [7]. All other chemicals were commercially available products, used without further purification. The degree of substitution of the hydroxypropyl derivatives of guar are defined hereinafter as “molar substitution” (m.s.), while, for the methoxylated guar derivatives, it is expressed as “degree of substitution” (d.s.). This distinction is appropriate because, in the former case, the molar number of hydroxypropyl substituents does not coincide with the number of substituted sites along the chain because of the possibility of the building up of side chains. In the latter case, the number of functionalized hydroxyls on guar backbone coincides with the number of moles of methyl groups introduced. The degree of substitution (d.s.) and molar substitution (m.s.) of guar derivatives were determined by ^{1}H NMR of partially degraded samples.

2.2. Light scattering measurements

Stock solutions of guar and guar derivatives were prepared by dissolving the polymers at the proper concentration in Na_2SO_4 electrolyte solution and then by dialyzing against Na_2SO_4, 55 mM, aqueous solution for 5 days, in a special cell at constant volume.

Static light scattering measurements were carried out in the angular range between 30° and 130° in steps of 5° with a computer driven goniometer Brookhaven Instruments Corp. mod. Bi 200SM equipped with a digital correlator BI-9000AT. The beam from a solid state laser 125 mW operating at 532 nm was focused onto the sample cell through a temperature controlled chamber (temperature controlled within ±0.05 °C), filled with a refractive index-matching liquid (decaline). All solutions were prepared in a laminar air flow cabinet to minimize dust contamination. The solutions were filtered through 0.45 μm Millipore filters, directly into pre-cleaned light scattering cuvettes (Pyrex disposable cultures tubes, Corning Inc. Corning NY) (total volume of 3 mL).

Weight-average molecular weight (M_w), z-average root-mean-square radius of gyration (R_g) and the second virial coefficient (A_2) were measured for all the samples investigated. These parameters were obtained from the appropriate Berry plots [8], by extrapolation of the experimental data to the concentration $C \rightarrow 0$ and the scattering vector $q^2 \rightarrow 0$.

2.3. Viscosity measurements

The viscosity η of the polymer solutions was measured by means of a unit AVS379 (Schott-Geräte, Hofheim, Germany), connected to a Viscodoser AVS20 piston burette (for automatic dilutions), to make automated measurements of the flow-through times in a capillary viscometer (Ubbelohde viscometer, $\Phi = 0.53$ mm). The viscometer was immersed in a precision water bath (transparent thermostat CT 1150, Schott-Geräte, Hofheim, Germany) to a constant temperature of 25.0 ± 0.1 °C. The solutions were prepared by dissolving liophilized samples under magnetic stirring for at least 24 h at room temperature, followed by filtration through a Millipore filter of 0.45 μm.

The intrinsic viscosity [η], was obtained by extrapolation to zero concentration of Huggins' and Kraemer's equations [9], respectively,

$$\frac{\eta_{sp}}{C} = [\eta] + k'\left[\eta^2\right]C \tag{1}$$

$$\frac{\ln(\eta_{rel})}{C} = [\eta] + k''\left[\eta^2\right]C \tag{2}$$

where $\eta_{rel} = \eta/\eta_s$ and $\eta_{sp} = (\eta - \eta_s)/\eta_s$ are the (dimensionless) relative and specific viscosities, k' and k'' are the Huggins' and Kraemer's coefficients, respectively, η_s the viscosity of the solvent and C is the polymer concentration.

2.4. Steady-shear flow measurements

Steady-shear experiments in solution of different concentrations (0.1–2.0% w/v) were performed with a double gap (DG) for low viscosity solutions and a cone and plate (CP 4/40) for solutions with a zero-shear viscosity larger than 600 mPa s of a Bohlin CS10 rheometer, version 4.033 and a temperature control bath (Bohlin Rheometer). For steady state studies, the shear rates investigated were in the range between 0.01 and 1000 s^{-1}. The waiting times among measurements taken at different stresses and the integration times were chosen to allow the system to reach a steady state. In no cases, viscosity exhibited time-dependent phenomena.

2.5. Oscillatory shear measurements

Oscillatory experiments were carried out by means of a Bohlin Rheometer using the same geometry as the one used in the steady-shear measurements. A sinusoidal strain wave with angular

frequency ω was applied to the upper plate and the response of the sample exerted on the same plate was detected by the transduction system. The viscoelastic properties, storage modulus $G'(\omega)$ and loss modulus $G''(\omega)$ were determined through small amplitude oscillating shear flows at angular frequencies ranging from 10^{-3} to 10 rad/s. Prior to any dynamic experiment, a strain sweep test at a constant angular frequency of 1 rad/s allowed to fix the upper limit of the viscoelastic zone at a strain value of 0.05%.

Both steady-shear stress viscosity and linear viscoelastic moduli measurements between 0.001 and 10 Hz were carried out at temperatures ranging from 10 to 80 °C. To avoid the effects of solvent evaporation, a thin layer of silicone oil was applied on top of the submerged bob.

3. Results and discussion

3.1. Analysis of static light scattering data

Polymer solutions were investigated by means of light scattering technique in the dilute concentration range from 0.2 to 0.8×10^{-3} g/dl, well below the critical concentration of coil overlap. The weight-average molar mass (M_w), the z-average root-mean-square radius of gyration (R_g) and the second virial coefficient (A_2) were obtained from the angular and concentration dependence of the excess absolute scattering intensity (Rayleigh ratio R_θ) in static laser light scattering measurements

$$\frac{KC}{R_\theta} = \frac{1}{M_w}\left(1 + \frac{1}{3} < R_g^2 > q^2\right) + 2A_2C \tag{3}$$

where $K = 4\pi n^2(\mathrm{d}n/\mathrm{d}C)^2/N\lambda^4$ and $q = (4\pi n/\lambda)\sin(\theta/2)$ with N the Avogadro number, $\mathrm{d}n/\mathrm{d}C$ the specific refractive index increment, n the solvent refractive index and λ the wavelength of the light in vacuum [10].

Usually, the scattering data are presented in the form of a Zimm plot [11] in which the ratio KC/R_θ is plotted against $q^2 + kC$ where k is an appropriate constant. The Zimm plot allows an easy extrapolation of the scattering data for both $\theta \to 0$ and $q \to 0$, giving the reciprocal molar mass.

However, this procedure requires caution, particularly for water-soluble polymers, because i) the concentration dependence of scattered light is not always linear; in some cases, its slope is so high that the intercept is very close to zero and often the extrapolation might even give a negative value; ii) for many water-soluble polymers, including polysaccharides, a complete molecular dispersion in solution is difficult, i.e. the solutions contain, in addition to individual macromolecules, also super-molecular structures. Even a very small amount of such aggregates can distort the angular dependence of scattered light in a quite characteristic fashion, producing a pronounced downturn in these data and consequently indicating a much higher molar mass.

In order to overcome these difficulties, the Berry plot [8] modification of the Zimm procedure is used to fit the light scattering data, according to the expression

$$\frac{KC}{R_\theta} = \frac{1}{M_w}(1 + A_2M_wC)^2 \tag{4}$$

Moreover, aggregation can be eliminated, or partially reduced, by chemical methods. For instance, non-covalent intermolecular association may be disrupted either by chemical modification of the polymer, or by use of a "denaturant" such as Na_2SO_4. Na^+ and SO_4^{-2} ions are known to bind water molecules extensively [12,13]. The interaction between Na^+ and SO_4^{-2} ions and the hydroxyl groups of guar and its derivatives should suppress the intermolecular hydrogen bonding and should prevent the formation of aggregates. As pointed out by Picout et al. [14], a disaggregating procedure has to be adopted in the case of guar-gum dissolved in water, in order to obtain a solution of true individual macromolecular species.

As an example, the Berry plots of MG and MHPG polymer aqueous solutions are shown in Fig. 1. The molar masses (M_w) together with the radius of gyration (R_g) and the second virial coefficient (A_2) for the four polymer solutions investigated are given in Table 1. The values of the molecular weights are in good agreement with those evaluated by means of viscometric methods [7].

As can be seen, the value of R_g of MG and MHPG polymers is remarkably lower than the one of GG polymer [14]. The introduction of methyl functionalities onto the GG backbone yields a notable reduction of the average macromolecular size. This is probably due to the reduction of the intermolecular and intramolecular hydrogen bond interactions, with a consequent reduction of both the number and the size of the aggregates, besides of the stiffness of the chains, as well.

As can be noted in Table 1, R_g of MHPG is very similar to the one of MG polymer, in spite of the fact that its molecular weight is about an half. This suggests that MHPG coils are more expanded than MG ones. This is in agreement with the values of C_∞ of MG and MHPG polymers previously determined (8.5 and 25.3, respectively) [7] and is coherent with the larger steric hindrance caused by the presence in MHPG polymer of mono and oligomeric hydroxypropyl substituents.

As mentioned, the second virial coefficients A_2 were also obtained from the fit of eq. (4) to the measured data. A_2 provides the strength of the interaction. A positive value of A_2 signifies an effective repulsive pair interaction between polymer chains, whereas a negative value suggests that the interaction is attractive in character.

The positive values of A_2 indicate that Na_2SO_4 aqueous solution is a good solvent for both MG and MHPG.

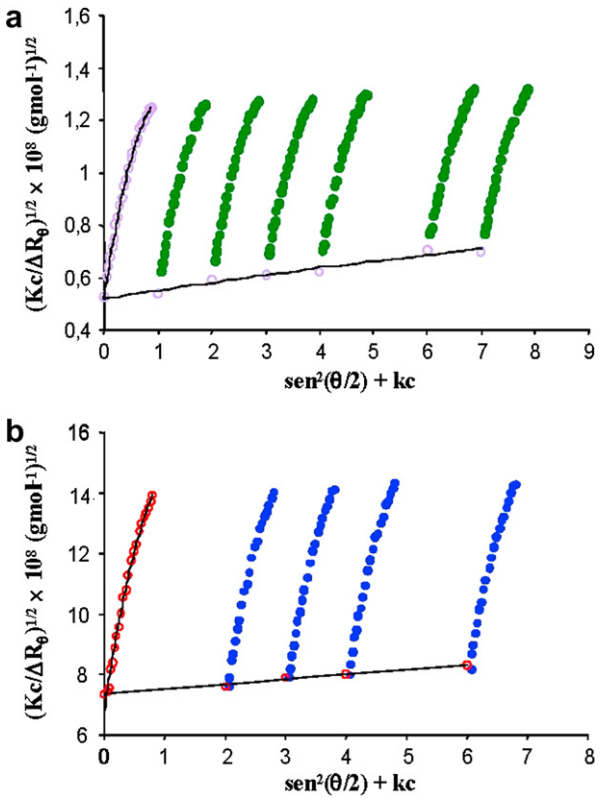

Fig. 1. Berry plot of MG d.s. = 0.3 (a) and of MHPG d.s. = 0.3, m.s. = 1.2 (b) polymers in Na_2SO_4, 55 mM, aqueous solutions, at the temperature of 40 °C.

Table 1
Average molecular weight, M_w, radius of gyration, R_g and second virial coefficient, A_2, for GG, MG, HPG and MHPG polymers in aqueous solution, at the temperature of 40 °C.

sample	$M_w \times 10^{-6}$	R_g [nm]	$A_2 \times 10^4$ [cm^3 mol/g]
GG	2.4	133	–
MG (d.s. = 0.3)	2.6	87.4	1.4
HPG (m.s. = 1.2)	5.0	–	−1.0
MHPG (d.s. = 0.4; m.s. = 1.2)	1.0	86.0	1.5

As far as HPG polymer is concerned, light scattering results evidence the presence of aggregates, which impair the correct determination of M_w and R_g of the individual coils (Table 1). The negative value of A_2 indicates that the solvent employed (Na_2SO_4, 55 mM) is not a good one for HPG. This polymer probably presents a structure with a balanced proportion of hydrophobic and hydrophilic domains, conferring to it a partial amphiphilic character. In a denaturing environment, the hydrophobic interactions prevail, leading to the formation of aggregates. This hypothesis was further confirmed by light scattering measurements of M_w and A_2 at temperature lower than 40 °C (data not shown). At temperatures of 10 and 20 °C, the contribution of aggregates to M_w is approximately constant, while A_2 has a less negative value than the one at $T = 40$ °C. Thus, the decrease of the temperature has the double effect of improving, to a some extent, the quality of the solvent but not enough to disaggregate the supramolecular entities. On the other hand, the perturbation due to the methyl groups in MG and MHPG polymers joined to the denaturing effect of Na_2SO_4 seems to be effective in preventing the hydroxyl groups from forming hydrogen bonds, even though the presence of some aggregates cannot be completely ruled out.

3.2. Analysis of viscosity and rheological data

3.2.1. Steady-shear properties

For dilute solutions, the non-Newtonian regime when the shear rate increases, is relatively small and is due to alignment and deformation of transiently elongated chains in the flow direction. At low shear rates, the disruption of entanglements by the imposed deformation is replaced by new interactions between different partners, with no net change in the entanglement density, and hence no reduction in the viscosity is observed. This situation corresponds to the horizontal "Newtonian plateau" in viscosity shear rate plots. For more concentrated solutions, shear thinning is much more dramatic and arises from an additional mechanism involving entanglements [15]. The onset of shear thinning occurs when the rate of externally imposed movements becomes greater than the rate of formation of new entanglements and thus the cross-link density of the network is depleted, and the viscosity consequently reduced.

The portion between these two behaviours corresponds to a transition region which depends on the molecular weight distribution, being larger and shifted towards the lower side for larger polydispersity [15].

Typical flow curves, at 25 °C, for guar and guar derivatives solutions at different polymer concentrations, are shown in Fig. 2.

The data can be conveniently described by the Cross equation [16]

$$\eta(\dot{\gamma}) = \eta_\infty + \frac{\eta_0 - \eta_\infty}{1 + (\tau\dot{\gamma})^n} \tag{5}$$

where η_0 and η_∞ are the limiting viscosities at zero and infinite shear rate, respectively, τ is the relaxation time and n an appropriate exponent.

Since, in our case, the experimental data are far from approaching the second (upper) Newtonian region, we have assumed η_∞ equal to the viscosity of water solvent at the given temperature ($\eta_\infty \simeq \eta_s = 0.893$ mPa s at $T = 25$ °C) [17].

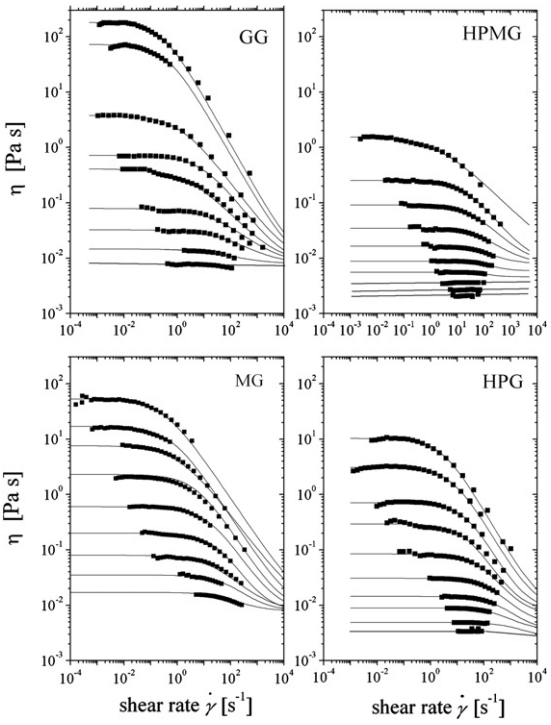

Fig. 2. Flow curves of GG, MG, HPG and MHPG polymers aqueous solutions as a function of the shear rate $\dot{\gamma}$, at the temperature of 40 °C. The full lines represent the calculated values according to the Cross equation (eq. (5)).

The parameters η_0, τ and n have been determined by means of a non-linear lest-squares fitting procedure of eq. (5) to the experimental data. The calculated behaviours, together with the measured values, are shown in Fig. 2. Different relaxation models, such as, for example, the Carreau model [18], $\eta(\dot{\gamma}) = \eta_0/(1 + (\tau\dot{\gamma})^2)^n$, which analogously allows the determination of the relaxation time τ and of the exponent n, does not furnish values of the parameters basically different.

The relaxation time τ from the apparent viscosity data can be also found on a pure phenomenological point of view, from the intersection of the constant Newtonian viscosity (measured at low shear rate) with the power law fit in the shear-thinning region (measured at higher shear rate). The dependence of τ on the polymer concentration C for the different polymer solutions investigated is shown in Fig. 3.

Scaling models based on the static correlation length ξ [19,20] predict dependencies like

$$\tau \simeq C^{1/4} \tag{6}$$

in the semidilute unentangled regime and

$$\tau \simeq C^{3/2} \tag{7}$$

in the semidilute entangled regime. As can be seen in Fig. 3, all the samples investigated behave as semidilute entangled solutions up to concentration in the range 0.5–0.8 g/dl, showing the predicted scaling. For higher concentrations, the data show a stronger concentration dependence, ($\tau \simeq C^{2.95\pm0.19}$), providing evidence for a concentrated regime. The cross-over concentration C^* between semidilute and concentrated regime lies, for all the systems investigated, in the range 0.5–0.8 g/dl, slightly different for the different polymers, in the order GG < MHPG < MG < HPG.

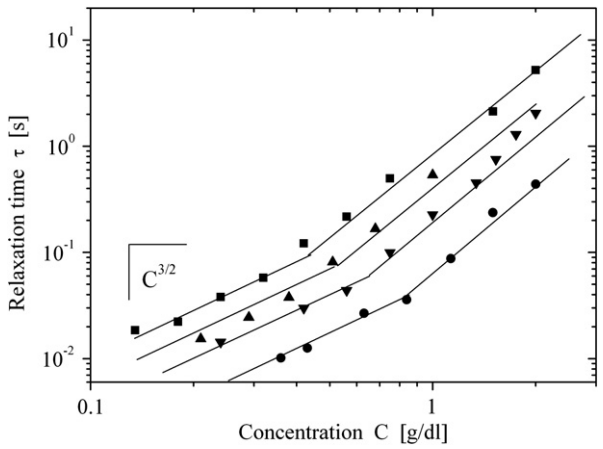

Fig. 3. Relaxation time τ as a function of the polymer concentration C for different guar and guar derivatives polymer solutions: (■): GG; (▼): MG; (●): HPG; (▲): MHPG. In the semidilute entangled regime, the data obey the scaling law $\tau \sim C^{3/2}$.

3.2.2. Specific viscosity and critical concentrations

The behaviour of guar and guar derivatives solutions have been investigated by analyzing the "zero shear" specific viscosity $\eta_{sp} = (\eta - \eta_s)/\eta_s$ as a function of the polysaccharide concentration, at the constant temperature of 25 °C.

A double logarithmic plots of η_{sp} against the concentration C is shown in Fig. 4, where are clearly evidenced the evolution from the semidilute (unentangled and entangled) to the concentrated regime, as the concentration C is increased.

At low polymer concentrations (dilute region), η_{sp} increased approximately linearly with increasing concentration, but at higher concentrations (entangled domain and concentrated regime), the slopes changed to much higher values. A similar behaviour is well known for solutions of many typical "random coil" polysaccharides [21] and it was attributed to the transition from the dilute regime, where individual polymer molecules are present as isolated coils, to a concentrated regime where the total hydrodynamic volume of the individual chains exceeds the volume of the solution.

The concentration C^* can be assumed as a boundary concentration between semidilute and concentrated regime where the individual coils start to entangle and give rise to significant coil overlap and interpenetration. The critical concentration C^* is sensitive to the intrinsic molecular properties of the polymer, such as chain stiffness and the solvent-polymer interaction.

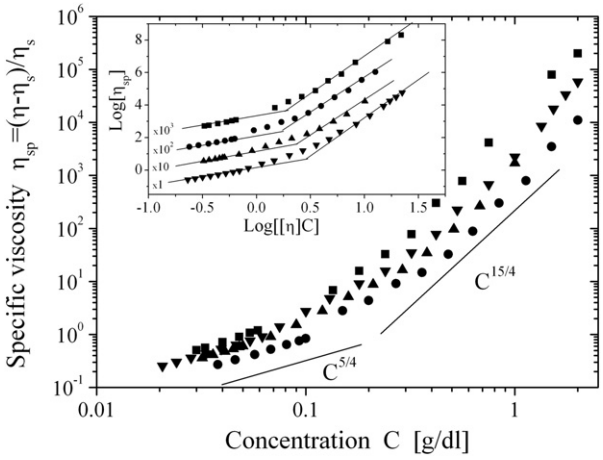

Fig. 4. Specific viscosity $\eta_{sp} = (\eta - \eta_s)/\eta_s$ as a function of the polymer concentration C for different guar and guar derivatives polymer solutions: (■): GG; (▼): MG; (●): HPG; (▲): MHPG. The dependencies $\eta \simeq C^{5/4}$ and $\eta \simeq C^{15/4}$ according to the scaling theory [19,20] are also shown. The insert shows in a double Log plot the dependence of $\eta_{sp} = (\eta - \eta_s)/\eta_s$ as a function of the product $C[\eta]$. For clarity of presentation, values of $\log[\eta_{sp}]$ are shifted one each other by a factor of ten.

For polymers of different primary structure but with similar conformational characteristics, it has been observed that, in the semidilute unentangled regime ($C < C_e$), the power law $\eta \sim C^{5/4}$ is in agreement with values found for all the samples investigated and, moreover, in agreement with those observed in a large number of polysaccharides [26,27], the range of slope values attained being relatively narrow (between 1.1 and 1.6). In the semidilute entangled regime ($C < C^*$), for most of the random coil polysaccharides interacting by purely topological entanglement, the scaling law $\eta \sim C^{15/4}$ is expected, according to the scaling theory, in a qualitative agreement with the dependencies $\sim C^{\gamma}$, with γ between 3.5 and 3.9, observed in the present case.

However, if η_{sp} is plotted against the (dimensionless) product of polymer concentration C (proportional to the number of chains present in the solution) and the intrinsic viscosity $[\eta]$ (proportional to the hydrodynamic volume of each chain), rather than against concentration C alone, the data for different polysaccharides superimpose closely regardless of polymer primary structure and molecular weight as shown in the inset of Fig. 4. As can be seen, two well-defined linear dependencies can be observed, both in the low and high concentration regime. The intersection of these two straight lines allows to estimate the dimensionless coil-overlap parameter $C^*[\eta]$, an index of the total volume occupied by all coils within the polymer solution, regardless of their molecular weight. These values estimated for the different polymers investigated are listed in Table 2. The $C^*[\eta]$ values of guar and guar derivatives are lower than those reported by Morris et al. [21] for other random coil polysaccharides, such as carboxymethyl cellulose, high mannuronan alginate, and λ-carragenan, but close to those for polysaccharides such as amilose ($C^*[\eta] = 1$ [22]), dextran ($C^*[\eta] = 0.8$–2.2 [23]), guar-gum ($C^*[\eta] = 1.0$) or locust bean gum ($C^*[\eta] = 1.3$ [24]).

The data obtained for guar and guar derivatives suggest that the process of chain entanglement and the formation of fully interpenetrated networks occur at higher concentration for MG and HPG polymers than GG and MHPG polymers, respectively (Table 2). This is probably due to the more expanded configuration (and, as a consequence, larger hydrodynamic volume [25]) of the chains in the latter type of polymers, as a result of their inherent rigidity (steric hindrance) and induced stiffness by intramolecular hydrogen bonds (especially in the case of GG polymer).

In the semidilute entangled regime, Heo and Larson [26,27], on the basis of the pioneering studies of Raspaud et al. [28], proposed a master curve yielding the power law

$$\frac{\eta - \eta_s}{\eta_{Rouse}} = K\left(\frac{C}{C_e}\right)^{\beta} \tag{8}$$

where η_{Rouse} is the hypothetical Rouse viscosity for a semidilute (entangled) polymer solution given by

Table 2
Exponents of the Cross equation n, intrinsic viscosity $[\eta]$, critical cross-over concentration C^*, coil-overlap parameter $C^*[\eta]$, energy of activation E_a, pre-exponential factor A for guar and guar derivatives aqueous solutions.

sample	n	$[\eta]$ [dl/g]	C^* [g/dl]	$C^*[\eta]$	E_a [kJ/mdK]	$A \times 10^4$
GG	0.21–0.63	8.5	0.25	1.91	25.7	9.8
MG (d.s. = 0.3)	0.085–0.21	8.5	0.35	2.95	28.1	2.0
HPG (m.s. = 1.2)	0.095–0.62	4.7	0.43	2.0	24.1	2.1
MHPG (d.s. = 0.4; m.s. = 1.2)	0.073–0.42	7.4	0.30	2.95	20.4	9.0

$$\eta_{\text{Rouse}} = \eta_s (C[\eta])^{1/(3\nu-1)} \quad (9)$$

with $[\eta]$ the intrinsic viscosity and ν the excluded volume exponent and C_e is the concentration at which entanglement effects begin. Heo and Larson [26], using data for a variety of polymer solutions, found $\beta = 3.12 \pm 0.05$. Fig. 5 shows that the data, for all the polymer solutions investigated, fall on the same master curve with a slope in very good agreement with the value predicted by Heo and Larson [26,27]. This result gives further support to the assignment of different regimes in the different concentration ranges.

Going back to the parameters of the Cross model, the exponent n was found to systematically change with concentration, ranging from 0.20 at low concentration to 0.65 at high concentration. Table 2 summarizes the values of the relevant parameters for the different guar and guar derivatives polymers solutions investigated.

From these data, it can be observed that, all concentrations being equal, i) MG and HPG polymer solutions present a lower viscosity than GG and MHPG solutions do, reflecting the difference in intrinsic viscosity $[\eta]$ of the samples, ii) the onset of shear-thinning behaviour appears at a higher shear rate for GG and HPG polymer solutions in comparison to MG and MHPG ones, respectively, the extent of this effect being more pronounced with the decrease of polymeric concentration, iii) GG and HPG polymers exhibited stronger shear-thinning properties in comparison to MG and MHPG polymers, as witnessed by their higher n values (Table 2) which rules the shear dependence in the power law region.

3.2.3. The effect of temperature

The dependence of the viscosity η on temperature T is described by the Arrhenius equation

$$\eta = A \exp(E_a/RT) \quad (10)$$

where A and E_a are the pre-exponential factor and the energy of activation, respectively, both of them dependent on the applied shear rate.

The energy of activation E_a decreases with the increase of the shear rate $\dot{\gamma}$. In the Newtonian plateau, the entanglement density among polymeric chains is independent of $\dot{\gamma}$ and E_a is constant. In the shear-thinning region, the entanglement density decreases constantly and a correspondingly lower and lower E_a value is necessary to set the solution under flux.

For the determination of E_a, measurements of η as a function of temperature T between 10 and 80 °C on solutions at a fixed polymeric concentration of 1.0% w/v were carried out. The Arrhenius parameters (eq. (10)) for solutions of guar and guar derivatives are listed in Table 2.

A higher E_a value means a more rapid change of viscosity with temperature [29]. In Fig. 6, the logarithm of the zero-shear-rate viscosity as a function of $1/T$ for guar and guar derivatives is shown. One notable feature is the presence in the MG and MHPG polymer behaviour of a downwards bent on the high T side (>60 °C). Since the observed η value at $T > 60$ °C is smaller than the one expected from the linear extrapolation of η_0 from the lower temperature regime, this means that MHPG, and in particular MG, undergo a transition from a relatively expanded conformation to a more compact one.

The origin of this effect can be due to the partially hydrophobic nature of MG and MHPG polymers, i.e., the increase of temperature is accompanied by a loss of the water of hydration and by the enhancement of the inter and intramolecular interactions, with a concomitant shrinkage of the coils.

It is worth noting that the extent of the bent is more accentuated in MG with respect to MHPG polymer. This may be accounted for by the bulkier mono and oligomeric hydrohypropyl substituents, that in MHPG polymer prevent the adoption of a more compact conformation, in comparison with MG polymer.

The activation energy E_a, which is sensitive to individual macromolecular interactions, takes into account the energy that is necessary to move individual macromolecules in an environment of surrounding macromolecules. From the data of Table 2, it is evident that GG, MG and HPG polymers displayed a higher dependence of viscosity on the temperature than MHPG polymer does. This is in agreement with the view of a network of intermolecular hydrogen bonds which are broken down by the increase of temperature. The lower value of E_a of MHPG polymers suggests that the polymer interacts mainly by means of physical entanglements.

One way to account for the temperature dependence of the dynamics of polymers by means the temperature-dependent viscosity is the so-called Williams–Landel–Ferry [WLF] equation [30]

$$\frac{\eta}{\eta_0} = \exp\left(A \frac{T - T_0}{T - T_c}\right) \quad (11)$$

where T_c is the Vogel temperature (where the free volume is zero) and η_0 is the viscosity at the reference temperature T_0. An example of the linearized WLF equation is shown in Fig. 7. As can be seen, despite of some scatters, all the data are fitted reasonably well by a straight line.

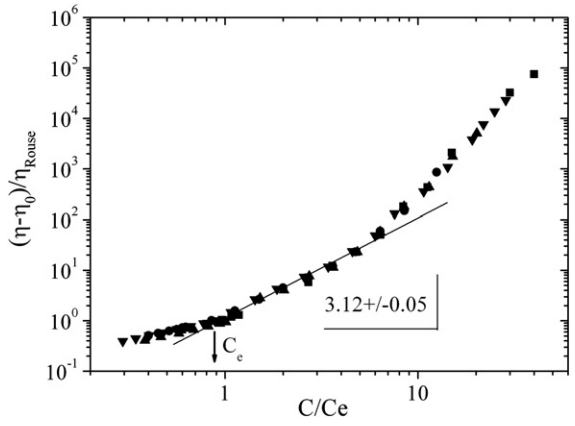

Fig. 5. Specific viscosity in the semidilute entangled regime as a function of C/C_e for different guar and guar derivatives aqueous solutions: (■): GG; (▼): MG; (●): HPG; (▲): MHPG. The data are well described by a scaling law with exponent 3.12, according to the Heo and Larson scaling.

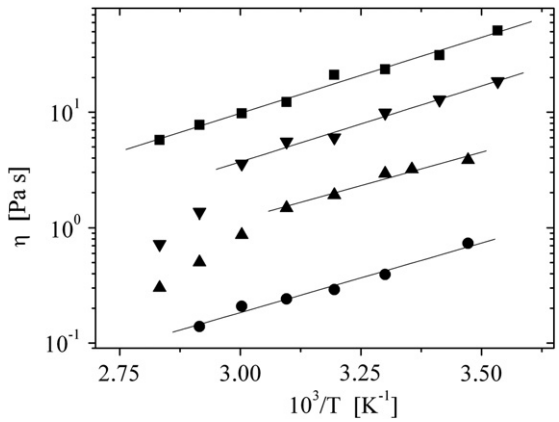

Fig. 6. Zero-shear-rate viscosity η as a function of inverse of temperature at a concentration of $C = 1.0\%$ w/v for different guar and guar derivatives polymer solutions: (■): GG; (▼): MG; (●): MHPG; (▲): HPG.

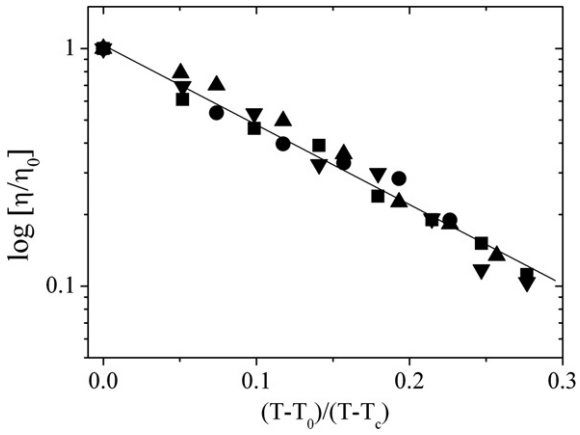

Fig. 7. The ratio η/η_0 as a function of the reduced temperature $(T-T_0)/(T-T_c)$ at a concentration of $C = 1.0\%$ w/v for different guar and guar derivatives polymer solutions: (■): GG; (▼): MG; (●): MHPG; (▲): HPG.

3.2.4. Rheological behaviour under dynamic shear

In order to characterize the viscoelastic behaviour of guar and guar derivatives aqueous solutions as a function of frequency, the dynamical spectra (complex moduli $G^*(\omega) = G'(\omega) + iG''(\omega)$) were measured at different polymer concentrations.

The moduli $G'(\omega)$ and $G''(\omega)$ are a quantitative measure of the elastic and viscous behaviour of the samples, their vectorial sum being proportional to flux resistance.

Fig. 8 shows the typical behaviour of the moduli $G'(\omega)$ and $G''(\omega)$ as a function of the angular frequency ω for guar and guar derivatives solution at the higher polymer concentrations investigated. In all the samples investigated, the behaviour of both $G'(\omega)$ and $G''(\omega)$ is typical of concentrated solutions.

At relatively low frequencies, $G'(\omega)$ is lower than $G''(\omega)$ and the response to imposed external strains is due to relative motion of the polymeric chains. As the frequency increases, the elastic component increases faster than the viscous one and, in such regime, solution behaviour turns from liquid-like to solid-like [30,31].

For frequency values above the intersection point, the elastic modulus overrates the viscous modulus, pointing out to a prevalence of intramolecular chain motions.

An increase of the polymeric concentration induces a shift of the intersection point between the two moduli, that can be defined as a cross-over point. As the polymeric concentration increases, the chain density of the network increases and motion of chain segments will undergo a correspondent decrease. This is due to longer relaxation times caused by restricted intramolecular motions and, to this effect, the decrease of the angular frequency at which $G' = G''$ is due.

A similar behaviour is generally observed with the increase of the molecular weight, at a constant polymer concentration [32]. For such reason, we will discuss separately the behaviour of GG and MG polymers and the one of HPG and MHPG polymers, which are characterized by very similar molecular weights (Table 1).

The inverse of the cross-over frequency can be seen as a characteristic time (denoted as $\tau_{G'=G''}$). The magnitude of $G'(\omega)$ at this point (denotes as $G'_{G'=G''}$) is an index of the characteristic strength of the relaxation spectrum, being proportional to the high-frequency storage modulus in the absence of Rouse relaxations. The coordinate of the cross-over point allows a further comparison among the polymers under analysis, since $G'_{G'=G''}$ is a function of the mass of the aggregates and $\omega_{G'=G''}$ is proportional to the degree of polydispersity of the aggregates.

From the analysis of the moduli behaviour as a function of the angular frequency ω (Fig. 8), we can deduce that the molar masses of the aggregates are in the order: GG > MG and HPG > MHPG and, analogously, the polydispersity is in the order GG < MG and HPG < MHPG. These indications confirm the hypothesis that the introduction of methyl groups onto chains prevents, to a some extent, the tendency of GG and HPG polymers towards aggregation and leads to a more heterogeneous system [32]. Moreover, the values of the angular dependence of $\omega_{G'=G''}$ as a function of concentration in the case of GG sample are in good agreement with literature data [32].

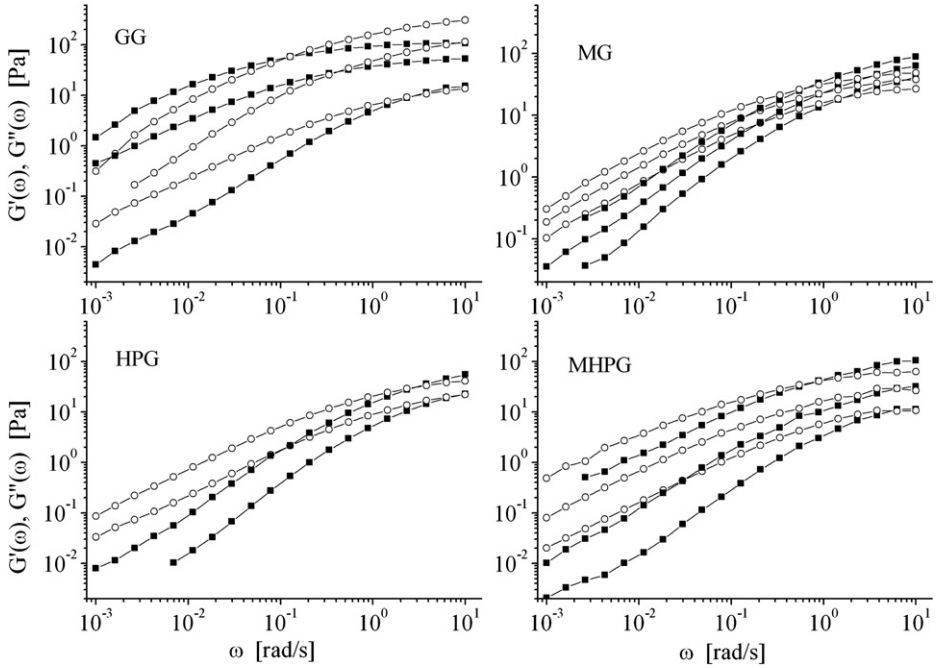

Fig. 8. Storage modulus $G'(\omega)$ (■) and loss modulus $G''(\omega)$ (○) as a function of angular frequency ω for guar and guar derivatives solutions, at different concentrations. GG: $C = 2.0$, 1.27, 0.75 w/v; MG: $C = 2.0$, 1.75, 1.53 w/v; HPG: $C = 2.0$, 1.5 w/v; MHPG: $C = 3.0$, 2.30, 1.73 w/v.

Considering the couple GG and MG polymers, it is evident that MG displays a lower dependence of $\tau_{G'=G''}$ on concentration, indicating a more compact conformation and a lower presence of hyper-entanglements and resulting in an enhancement of particle mobility. Similar considerations apply to HPG and MHPG polymer solutions.

The frequency dependence of the dynamic loss angle $\tan\phi = G''(\omega)/G'(\omega)$, which provides a measurement of the ratio of the energy dissipated as heat and the one stored during a cyclic deformation, decreases with the increase of the angular frequency ω. Typical examples for guar and guar derivatives solutions at different polymer concentrations (in the region of semidilute entangled and concentrated regime) are given in Fig. 9.

The observed behaviour can be justified by the enhanced contribution of the elastic component at higher frequencies with respect to the viscous one. In the whole range of angular frequencies ω investigated, the values of $\tan\phi$, at the same concentration, follows the order: MHPG < HPG < MG < GG. Low values of $\tan\phi$ indicate a solid-like solution structure. On the contrary, when $\tan\phi$ increases, the system behaves as a Newtonian fluid. Thus, GG solution seems to be characterized by a more extended network of interacting polymer chains which confers to this system a more pronounced solid-like behaviour than the one present in the derivative systems. As the hindrance and the number of substituents along the chain increase (as in MG and HPG polymer solutions) and the density of hydroxyl groups is reduced (as in MHPG polymer solution), $\tan\phi$ increases with the decrease of the angular frequencies ω more and more steeply, indicating essentially a lack of structure in the solution.

Complex viscosities of guar and guar derivatives aqueous solutions at various polymer concentrations are shown in Fig. 10 as a function of the angular frequency ω. For all the systems investigated, these results show that the dynamic viscosity η' approaches the apparent viscosity at low frequency and low shear rate, respectively. With the increase of both the frequency and shear rate, apparent and dynamic viscosity began gradually to diverge, with the expected more rapid decrease of dynamic viscosity with frequency than the apparent viscosity with shear rate. This can be attributed to the very different molecular motions involved in the dynamic and steady shear, at higher frequency and higher shear rate [30], respectively. With the increase of concentration of guar and guar derivatives, the dynamic viscosity became more divergent as shown in Fig.10. The complex viscosity is lower than the steady-shear viscosity over a wide shear rate/frequency domain. This type of behaviour has been reported for many associating polymer systems that display shear-thinning effects. Simulation studies of associating polymer systems [33,34] have revealed that the cross-link dissociation rate increases with the increase of the shear rate and shear forces may induce dramatic structural re-organizations of the network [35–37]. It is possible that, in strongly entangled solutions, the topological constraints are strengthened when

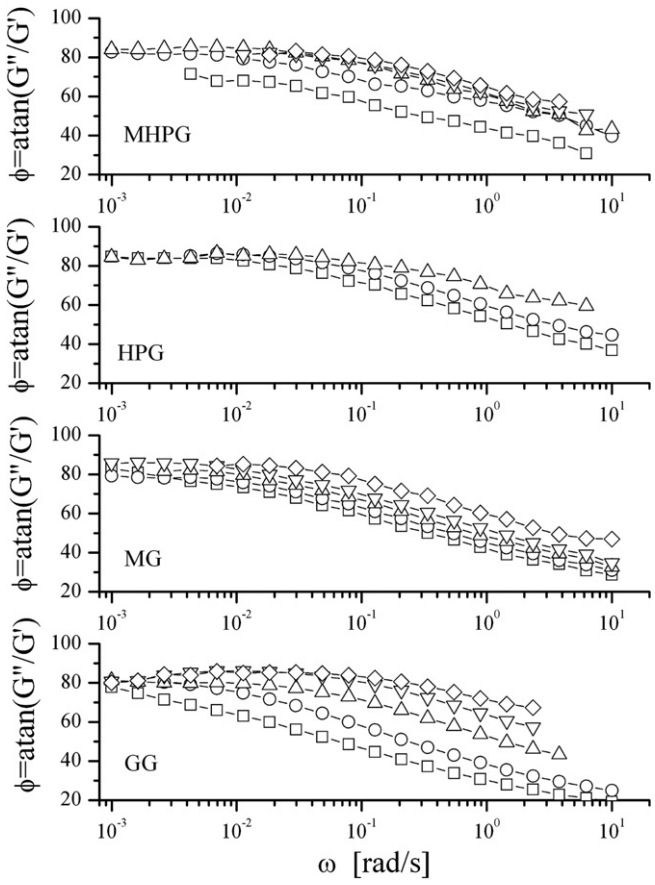

Fig. 9. Phase angle $\phi = \tan^{-1}(G''(\omega)/G'(\omega))$ as a function of angular frequency ω of guar and guar derivatives solutions at different concentrations. GG: (□) $C = 2.0$ w/v; (○): $C = 1.27$ w/v; (△): $C = 0.75$ w/v; (▽): $C = 0.56$ w/v; (◇): $C = 0.42$ w/v. MG: (□): $C = 2.0$ w/v; (○): $C = 1.75$ w/v; (△): $C = 1.53$ w/v; (▽): $C = 1.34$ w/v; (◇): $C = 1.9$ w/v. HPG: (□): $C = 2.0$ w/v; (○): $C = 1.50$ w/v; (△): $C = 1.13$ w/v. MHPG: (□): $C = 3.0$ w/v; (○): $C = 2.30$ w/v; (△): $C = 1.73$ w/v; (▽): $C = 1.51$ w/v; (◇): $C = 1.32$ w/v.

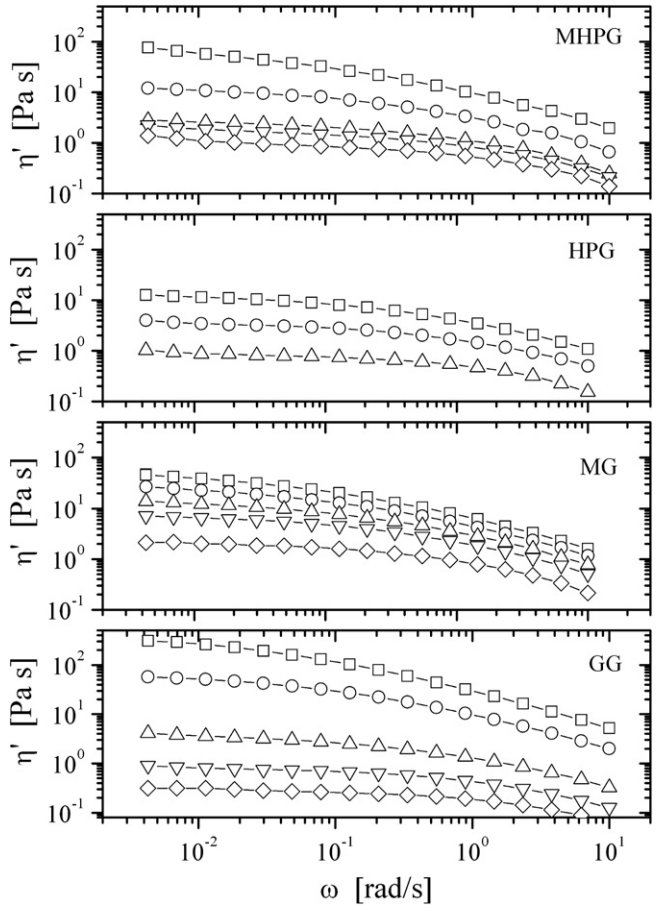

Fig. 10. Complex viscosity as a function of angular frequency ω of guar and guar derivatives solutions at different concentrations. GG: (□): $C = 2.0$ w/v; (○): $C = 1.27$ w/v; (△): $C = 0.75$ w/v; (▽): $C = 0.56$ w/v; (◇): $C = 0.42$ w/v. MG: (□): $C = 2.0$ w/v; (○): $C = 1.75$ w/v; (△): $C = 1.53$ w/v; (▽): $C = 1.34$ w/v; (◇): $C = 1.9$ w/v. HPG: (□): $C = 2.0$ w/v; (○): $C = 1.50$ w/v; (△): $C = 1.13$ w/v. MHPG: (□): $C = 3.0$ w/v; (○): $C = 2.30$ w/v; (△): $C = 1.73$ w/v; (▽): $C = 1.51$ w/v; (◇): $C = 1.32$ w/v.

moderate shear rates are imposed on the system, while oscillatory shear does not produce this effect.

Finally, we go back to the scaling of the moduli. As the polymer concentration increases and exceeds the entanglement concentration, the dynamic of the polymer is controlled by the size ξ of the correlation blob, the number n_e of the correlation blob per entanglement strand and by the time τ_e required for a molecule filling one "tube segment" to relax [38]. In this context, one can use ξ and n_e to normalize the modulus and τ_e to normalize the frequency. This constant time τ_e corresponds to the Rouse relaxation time of an entanglement strand. Since, the quantity $n_e\xi^3$ is related to the plateau modulus of a semidilute solution by the relation $G_N^0 = K_BT/(n_e\xi^3)$ [39], the effective scaling parameters are G_N^0 and n_e.

The plateau modulus is generally obtained from the area under the terminal loss peak [40,41]

$$G_N^0 = \int_0^\infty G''(\omega)\, \mathrm{dln}(\omega) \tag{12}$$

Since our measurements do not extend to higher enough frequencies, we assume, as suggested by Raju et al. [42], a direct proportionality to the loss modulus maximum, $G_N^0 = aG_m''$, in which the proportionality constant a assumes a value in the range $a = 3.0-4.0$.

We have compared rheological data of guar and guar derivatives solutions using $\tau_{e,scaling}$ as a relative equilibrium time for different measurements at different concentrations and molecular weights. We have appended the subscript "scaling" to τ_e in order to assign to this parameter a pure phenomenological meaning. This operation translates into a shift along the frequency axis and allows the construction of master curves over a wider range of frequencies.

The experimental normalized complex moduli $G'(\omega)/G_N^0$ and $G''(\omega)/G_N^0$ against $\tau_{e,scaling}$ plots are shown in Fig. 11. As can be seen, we have an excellent collapse with only slight discrepancies in the region of low frequencies, indicating a gradual breakdown of the scaling based on the blob model in the semidilute regime. Similar findings were also observed by Heo and Larson [38] on polystyrene solutions in tricresyl phosphate at different concentrations and molecular weights. However, all together, collapses shown in Fig. 11 give support to a *universal scaling* of rheological properties of semidilute to concentrated polymer solutions based on the "blob" model and the Colby–Rubinstein model [43].

3.2.5. Scaling with temperature

The time–temperature superposition [tTS] principle relates the frequency dependence of the complex modulus $G^*(\omega)$ at any temperature T to that of any reference temperature T_0 allowing its determination from a master curve. At each temperature T, a single frequency scale shift factor a_T and a single modulus scale shift factor b_T allow superposition of all viscoelastic data at temperature T with data at the reference temperature T_0, according to the relationship

$$G^*(\omega, T) = b_T G^*(a_T\omega, T_0) \tag{13}$$

This analysis can be carried out by means of two different steps, first, the shift of the loss tangent $\tan\phi = G''(\omega)/G'(\omega)$ on the frequency scale allows to determine a_T and then an independent modulus scale shift determines b_T.

As pointed out by Pathak et al. [44], in order to ensure that the modulus scale shift factor does not produce a false superposition, it is preferable to scale the loss tangent $\tan\phi = G''(\omega)/G'(\omega)$ so that any shift factor will be automatically cancelled. The temperature dependence of the frequency scale shift factor a_T required to shift the data from T to T_0 is empirically described by the WLF equation

$$\log a_T = -A\left(\frac{T - T_0}{T - T_g}\right) \tag{14}$$

where T_g is the Vogel temperature, where the viscosity diverges.

This technique holds if the supermolecular structure does not change and no conformational transitions occur upon changing the temperature.

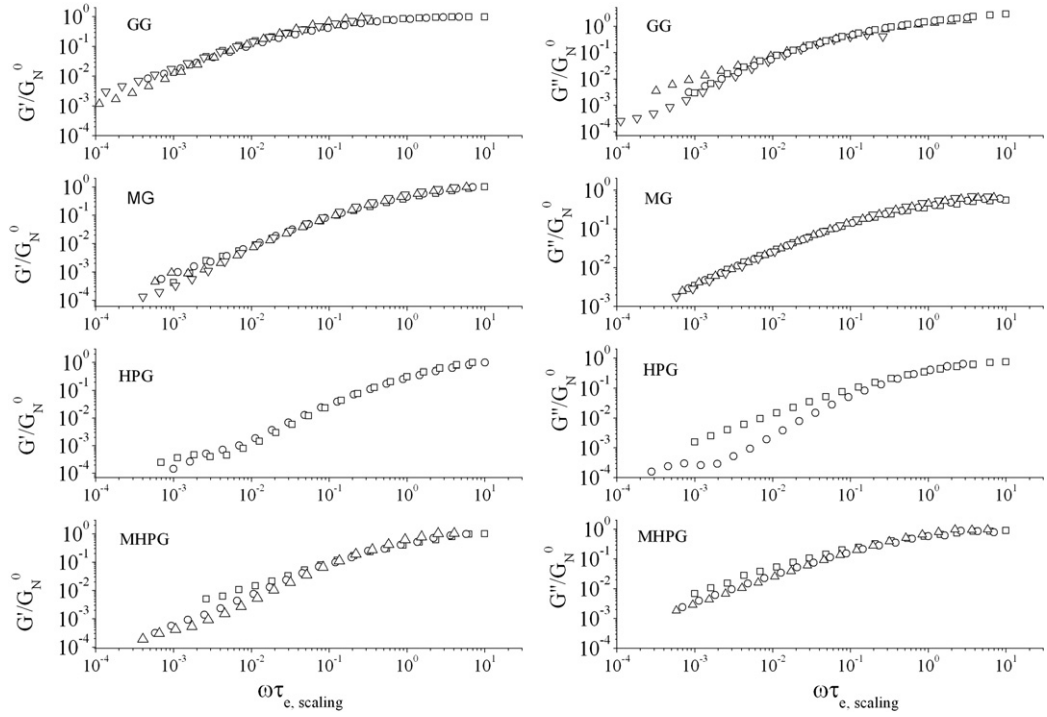

Fig. 11. Plots of the *universal scaling* of the linear viscoelastic properties of guar and guar derivatives aqueous solutions. In each plot, normalized storage and loss moduli $G'(\omega)/G_N^0$ and $G''(\omega)/G_N^0$ are plotted against the normalized frequency $\tau_{e,scaling}$ at different concentrations. GG: (□): 2 w/v; (○): 1.27 w/v; (△): 0.75 w/v; (▽): 0.56 w/v. MG: (□): 2 w/v; (○): 1.75 w/v; (△): 1.53 w/v; (▽): 1.34 w/v. HPG: (□): 2 w/v; (○): 1.50 w/v. MHPG: (□): 3 w/v; (○): 2.30 w/v; (△): 1.73 w/v.

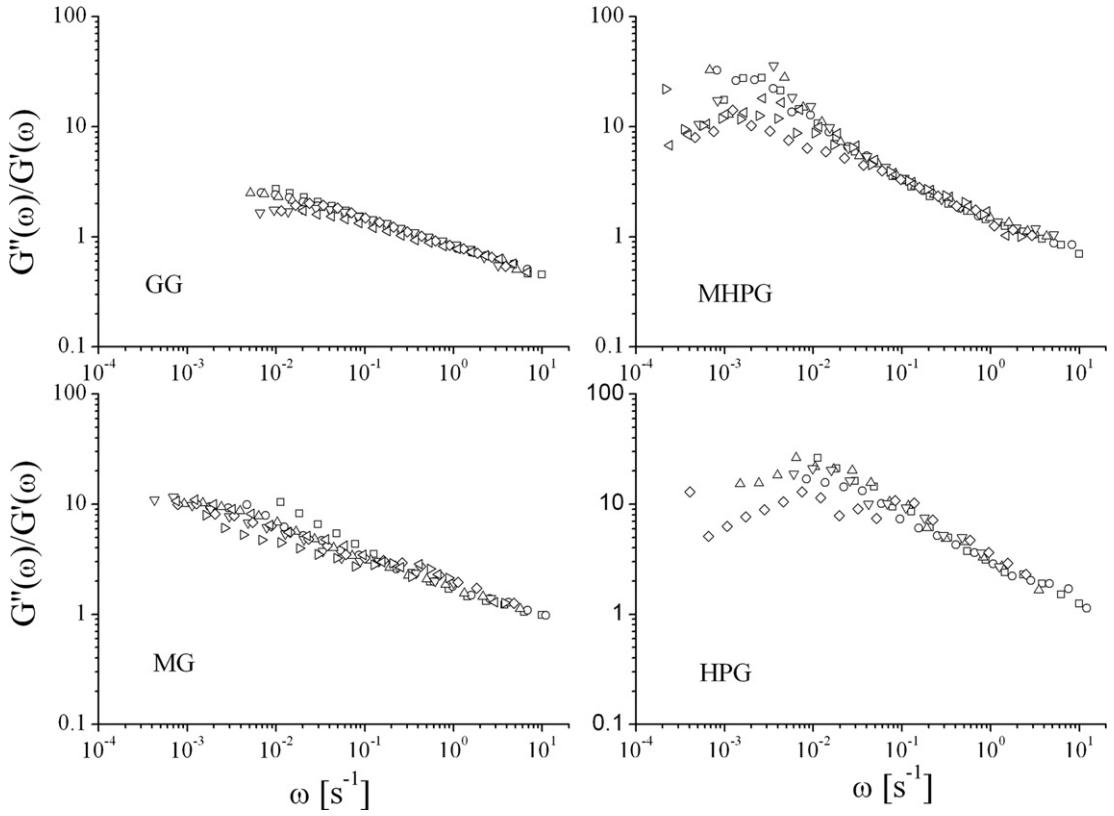

Fig. 12. Master curve showing the ratio $G'(\omega)/G''(\omega)$ as a function of the angular frequency according to the time–temperature superposition principle, for guar and guar derivatives at different temperatures: GG: (◇): 9.8 °C; (△):20.1 °C; (▽):30.1 °C; (◁):40.3 °C; (△):50.0 °C; (○):60.0 °C. MG: (◇):10.0 °C (△):20.0 °C; (▽):30.0 °C; (◁):40.0 °C; (▷):50.0 °C; (○):60.0 °C; (□):70.0 °C; (0):80.0 °C. HPG: (◇):15.0 °C; (△):25.0 °C; (▽):30.0 °C; (◁):40.0 °C; (▷):50.0 °C (○):60.0 °C; (□):70.0 °C; (0):80.0 °C. MHPG: (◇):15.0 °C; (△):25.0 °C; (▽):30.0 °C; (◁):40.0 °C; (▷):50.0 °C; (○):60.0 °C.

We have measured the rheological properties of guar and guar derivatives solutions in a wide temperature interval between 10 and 80 °C and time–temperature superposition method was employed in the analysis of the data.

Fig. 12 shows the master curves for guar and guar derivatives aqueous solutions for $G''(\omega)/G'(\omega)$ as a function of the angular frequency ω. A reference temperature of 10 °C was used in all cases. As can be seen, whereas all the data collapse over a unique scaling curve, it becomes evident that, in the low frequency side, both the storage modulus and the loss modulus, i.e., their ratio, show a different temperature dependence. To this respect, a quite different trend is observed for the couple GG/MG polymers from the HPG/MHPG polymers.

In the first case, deviations are relatively small. On the contrary, as far as the couple HPG/MHPG polymers is concerned, curves at different temperatures fail to superpose on a broad range of frequencies and, moreover, the variation of $G'(\omega)$ in such a region is not linear with the increase of temperature. In the temperature range between 10 and 60 °C, $G'(\omega)$ tends to increase linearly, whereas, beyond 60 °C, it decreases (data not shown). A lack of superposition is indicative of temperature-dependent relaxation mechanisms that occur within the material. This kind of behaviour is typically found in crystalline materials, polymers blends and multi-component systems, where relaxation behaviour changes with temperature [45]. The loss modulus of GG and MG polymers do not show these deviations in the scaling behaviour with temperature, while MHPG and in particular HPG polymer exhibits some deviations.

The behaviour of $G'(\omega)$ can be justified considering the activation energy E_a in the steady state experiments. It was found that, above about the temperature of 60 °C, MG and MHPG polymers underwent a re-organization of the solution structure, as witnessed by the abrupt decrease in the viscosity.

This finding suggests that, at a microscopic level, the polymer assumes, due to the hydrophobic effect, a multi-phase structure, whose relaxation times are affected differently by changes in temperature in the oscillatory experiments. In the range 10–60 °C, the polymers, driven by hydrophobic interactions, organize themselves into a network structure characterized by increasingly

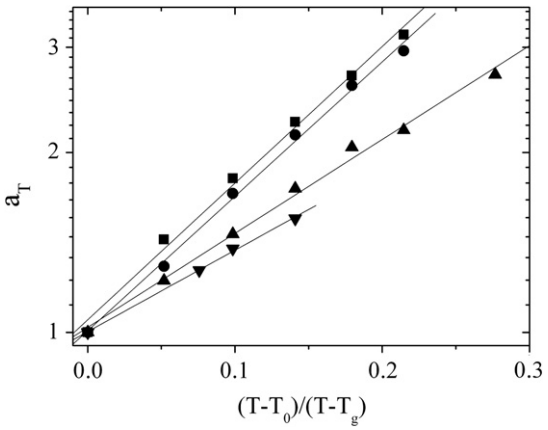

Fig. 13. The dependence of the frequency scale shift factor on the reduced temperature $(T - T_0) = (T - T_c)$ for guar and guar derivatives: (■): MG; (●): GG; (▲): HPG; (▼): MHPG.

solid-like rheological properties. For temperatures higher than 60 °C, the network collapses into individual aggregates and viscous properties become again predominant.

Finally, the temperature dependence of the frequency scale shift factor a_T for guar and guar derivatives solutions is shown in Fig. 13 along with their apparent fit to eq. (14). As can be seen, each sample investigated is characterized by a different slope in the dependence of a_T on the scaled temperature. Within the free volume model [46], the factor a_T is related to the fractional free volume f and its value f_g at the temperature T_g through the relation

$$a_T = \exp\left(\frac{a}{f} - \frac{a}{f_g}\right) \tag{15}$$

where a is a dimensionless parameter of order unity. Plot shown in Fig. 13 suggests that fractional free volume stays in the order HPG > MHPG > GG > MG.

4. Conclusions

We have measured the viscosity and the rheological properties of aqueous solutions of guar and guar derivatives in an extended polymer concentration range (over the semidilute and concentrated regime) and in the temperature interval from 10 to 80 °C. The influence of different substituents, methyl, hydroxypropyl and mixed derivatives, on the viscoelastic properties of guar solutions has been investigated.

The main results can be summarized as follows: i) guar and guar derivatives solutions show a moderate propensity to aggregate, as evidenced by light scattering measurements. This feature is particularly pronounced in the case of HPG polymer in the solvent system employed. ii) rheological measurements in steady-shear flow allowed the determination of the coil-overlap concentration C^*. The dependence of the Cross parameters η_0 and τ on polymer concentration is in reasonable agreement with the scaling predictions near the concentration onset of the entanglements. These scaling laws are satisfied independently of the typology and the extent of substitution. The flow behaviour as a function of temperature evidenced the partial hydrophobic nature of MG and MHPG polymers. These derivatives underwent a conformational transition from a relatively expanded to a more compact conformation. iii) the linear viscoelastic behaviour of guar and guar derivatives over an extended range of concentration and temperatures obeys both the concentration–time and temperature–time superposition principle and allows the construction of a universal master curve. Small deviation of the elastic modulus in the time–temperature superposition has been observed, in particular in the case of MG and MHPG polymer solutions, in the low frequency range, suggesting the presence of a supermolecular structure driven by hydrophobic interactions.

Acknowledgements

The authors thank La Sapienza, University of Rome (Ateneo funds) and MIUR (PRIN-2008) for financial support.

References

[1] McCleary BV, Clark AH, Dea ICM, Rees DA. Carbohydr Res 1985;31:241.
[2] Cheng Y, Prud'homme R, Chick J, Rau D. Macromolecules 2002;35:10155.
[3] Burke M, Park J, Srinivasarao M, Khan S. Macromolecules 2000;33:7500.
[4] Clourasia M, Jain S. Drug Deliv 2004;11:129.
[5] Murthy S, Hiremath S, Paranjothy K. Int J Pharm 2004;11:129.
[6] Zhang ML, Zhou JF, Hui PS. J Sci Food Agric 2005;85:2638.
[7] Risica D, Dentini M, Crescenzi V. Polymer 2006;46:12247.
[8] Berry GC. J Phys Chem 1966;44:4550.
[9] Kulicke WM, Clasen C. Viscosity of polymers and polyelectrolytes. Springer; 2004.
[10] Schmitz KS. An introduction to dynamic light scattering by macromolecules. Academic Press; 1990.
[11] Tanford C. Physical chemistry of macromolecules. New York: Wiley; 1961.
[12] Schott H, Royce AE. J Pharm Sci 1984;73:79.
[13] Royce AE, Han SK. J Colloid Interf Sci 1984;98:196.
[14] Picout DR, Ross-Murphy SB, Errington N, Harding SE. Biomacromolecules 2001;2:1302.
[15] Grassely WW. Adv Polym Sci 1974;16:1.
[16] Cross MM. J Colloid Interf Sci 1965;20:417.
[17] Lide DR. Handbook of chemistry and physics. 78th ed. CRC Press; 1998.
[18] Carreau PJ. Trans Soc Rheol 1972;16:99.
[19] Dobrynin AV, Colby RH, Rubinstein M. Macromolecules 1995;28:1859.
[20] Rubinstein M, Colby RH, Dobrynin AV. Phys Rev Lett 1994;73:2776.
[21] Morris ER, Cutler AN, Ross-Murphy SB, Rees DA. Carbohydr Polym 1981;1:5.
[22] Ellis HS, Ring SG. Carbohydr Polym 1985;5:201.
[23] Sabati J, Choplin L, Doublier JL, Arul J, Paul F, Monsan P. Carbohydr Polym 1988;9:287.
[24] Doublier JL, Launay B. J Texture Stud 1981;12:151.
[25] Kulicke WM, Keniewske R. Rheol Acta 1984;23:75.
[26] Heo V, Larson RG. Macromolecules 2005;49:1117.
[27] Heo V, Larson RG. J Rheol 2007;51:1099.
[28] Raspaud E, Lairez D, Adam M. Macromolecules 1995;28:927.
[29] Medina-Torres L, Brito-De la Fuente E, Torrestiana-Sanchez B, Katthain R. Food Hydrocolloids 2000;14:417.
[30] Ferry JD. Viscoelestic properties of polymers. 3rd ed. New York: Wiley; 1980.
[31] Ross-Murphy SB. In: Ross-Murphy SB, editor. Physical techniques for the study of food biopolymers. Glasgow, UK: Blackie Academic Professional; 1994. p. 342–92.
[32] Wientjes RHW, Duits MHG, Jongschaap RJJ, Mellema J. Macromolecules 2000;33:9594.
[33] English RJ, Gulati HS, Jenkins RD, Khan SA. J Rheol 1997;41:1163.
[34] Groot RD, Agterof WGM. Macromolecules 1995;28:6284.
[35] Khalatur PG, Khokhlov AR, Mogolin DA. J Chem Phys 1998;109:9602.
[36] Lund R, Lauten RA, Nystrm B, Lindman B. Langmuir 2001;17:8001.
[37] Khalatur PG, Khokhlov AR, Kovalenko JN, Mogolin DA. J Chem Phys 1999; 110:6039.
[38] Heo, T.; Larson, R.G., Macromolecules, 2008, 41, 8903.
[39] Doi M, Edwards SF. The theory of polymer dynamics. New York: Oxford, University Press, Inc.; 1986.
[40] Fetters LJ, Lohse DJ, Richter D, Witten TA, Zirkel A. Macromolecules 1994; 27:4639.
[41] Kannan RM, Lodge TP. Macromolecules 1997;30:3694.
[42] Raju VR, Menesez EV, Marin G, Graessley WW, Fetters LJ. Macromolecules 1981;14:1668.
[43] Rubinstein M, Colby RH. Polymer physics. Oxford Univ. Press; 2003.
[44] Pathak JA, Colby RH, Floudas G, Jerome R. Macromolecules 1999;32:2553.
[45] Groot RD, Agterof WGM. J Chem Phys 1994;100:1649.
[46] Pathak JA, Colby RH, Kamath SY, Kumar SK, Stadler R. Macromolecules 1998; 31:8998.